

High-Q bismuth silicate nonlinear glass microsphere resonators

Pengfei Wang^{1,2*}, Ganapathy Senthil Murugan¹, Timothy Lee¹, Ming Ding¹, Gilberto Brambilla¹,
Yuliya Semenova², Qiang Wu², Fumihito Koizumi³ and Gerald Farrell²

¹Optoelectronics Research Centre, University of Southampton, Southampton SO17 1BJ, United
Kingdom

²Photonics Research Centre, Dublin Institute of Technology, Kevin Street, Dublin 8, Ireland

³Technology Management Group, Asahi Glass Co., Ltd., Yokohama, 221-8755, Japan

Abstract: The fabrication and characterization of a bismuth-silicate glass microsphere resonator has been demonstrated. At wavelengths near 1550 nm, high-Q modes can be efficiently excited in a 179 μm diameter bismuth-silicate glass microsphere via evanescent coupling using a tapered silica fiber with a waist diameter of circa 2 μm . Resonances with Q-factors as high as 0.6×10^7 were observed. The dependence of the spectral response on variations in the input power level was studied in detail to gain an insight into power-dependent thermal resonance shifts. Because of their high nonlinearity and high-Q factors, bismuth-silicate glass microspheres offer the potential for robustly assembled fully integrated all-optical switching devices.

* Corresponding author: pw3y09@orc.soton.ac.uk

1. Introduction

Over the last few decades, microsphere resonators have increasingly attracted interest because they have the potential to become key components in a variety of active and passive photonic circuit devices, offering a range of significant functionalities to planar lightwave circuits such as feedback, wavelength selectivity, energy storage to allow dispersion control, enhanced nonlinearity, resonant filtering, and ultralow threshold lasing [1]. The use of glass microsphere resonators in photonic circuit devices offers great flexibility in terms of material composition and properties such as nonlinearity and gain.

Nonlinear optical materials have been exploited for the direct implementation of several key functions such as wavelength conversion, optical switching and signal regeneration, which have the potential to radically transform future optical communication networks. Most studies on microsphere resonators have utilized silica microspheres fabricated by melting the tip of an optical fiber with the resulting stem used as a tool to position the sphere while it is being characterized [2]. Microresonators realized from highly nonlinear chalcogenide glasses have recently been studied because of their high optical nonlinearity [3,4]. We have recently fabricated a nonlinear lead-silicate fiber-based microsphere resonator and showed that the supported ultra-high Q WGMs have properties close to their theoretical limit [5].

Bismuth-silicate ($\text{SiO}_2\text{-Bi}_2\text{O}_3$) glass has a nonlinear refractive index n_2 that can be as high as 17 times that of conventional silica [6]. Compared with other highly nonlinear compound glasses, bismuth glasses do not contain toxic elements such as Pb, As, Se, Te [7]; and most importantly nonlinear fibers made from bismuth silicate glass can be fusion-spliced to silica fibers [8], which allows for easy integration with conventional silica fiber based optical systems. Furthermore, bismuth silicate fibers exhibit good mechanical, chemical and thermal stability, low-loss and high nonlinearity, allowing for the observation of strong nonlinear effects, including supercontinuum

generation [9,10], four wave mixing [11], switching [12-14] and parametric amplification. In this paper, a nonlinear glass microsphere resonator is fabricated from a bismuth-silicate fiber using resistive heating; whispering-gallery modes with Q factors up to 0.6×10^7 are observed and the dependence of the spectral response of the whispering-gallery modes upon input power is studied to clarify the effects of thermal nonlinearity.

2. Theoretical analysis of bismuth silicate glass microspheres coupled with a silica fiber taper

Based on the comprehensive theoretical investigation for analyzing microsphere resonator excitation presented in Ref. [15], Fig. 1 compares the effective index (n_{eff}) of the 1550 nm fundamental HE_{11} mode of the fiber taper with those of microsphere WGMs for different sphere sizes, showing the 6 lowest radial order WGMs for $l=m$ where the order of l is chosen so the resonant wavelength is ~ 1550 nm. The refractive index of the tapered fiber was taken to be 1.444 while the refractive index of the microsphere was taken to be 2.01. The higher order (high n) radial modes (and also higher order Hermite-Gaussian modes with $m < l$) have an n_{eff} closer to that of the mode propagating in the fiber taper than the fundamental WGM mode ($n=1$), thus they can be excited more efficiently than the fundamental WGM. In fact, coupling efficiency is strongly related to the phase mismatch, thus modes which have smaller phase mismatch experience stronger coupling.

In the simulations carried out to evaluate n_{eff} of the bismuth silicate microsphere WGMs, the values of l (such that $l=m$) for each point were chosen to keep the resonant wavelength close to 1550 nm. The higher order modes ($n \gg 2$) have a lower l and m values, hence a lower n_{eff} . Furthermore the resonance spectrum is likely to be complicated by the non-degeneracy of the aforementioned Hermite-Gaussian modes with a different order m , due to the ellipticity observed in fabricated microspheres.

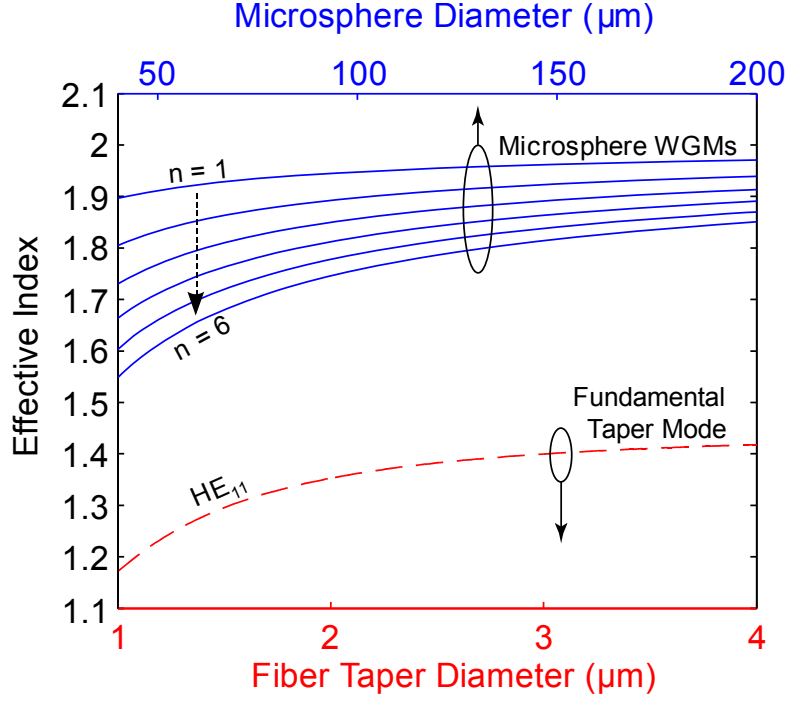


Figure 1. Effective index at $\lambda = 1550$ nm for the fundamental mode of a silica fibre taper with diameter d in the range 1-4 μm (red dashed line) and whispering gallery modes in a bismuth silicate microsphere for different sphere sizes (blue solid lines). The latter are calculated for radial mode numbers $1 \leq n \leq 6$ and $m = l$, where l is the azimuthal mode number and m is the polar mode number, l is chosen to provide resonances at ~ 1550 nm.

To better illustrate the whispering-gallery modes propagating within the bismuth silicate microsphere, the electric field of the high order WGMs are calculated and plotted in Fig. 2 (a) and (b) for a microsphere with the same properties as those used in the experiments (Section 3), using the theory presented in Ref. [15]. The field near the surface is weak since the mode resides up to 5 μm beneath the interface, due to the strong modal confinement arising from the high index contrast. It is therefore important to optimise the distance between the taper and the sphere to maximise coupling.

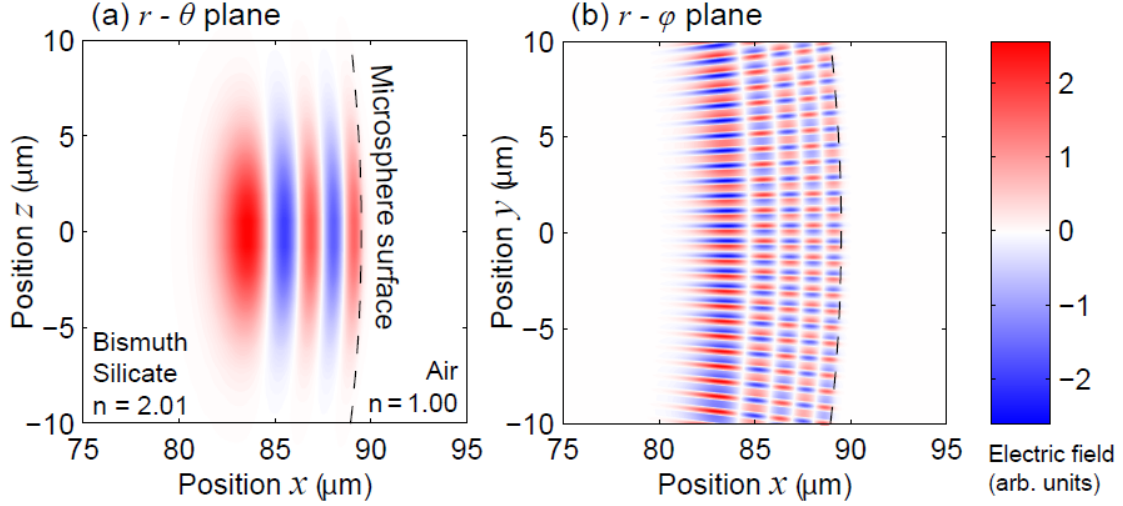


Figure 2. A higher order WGM for a bismuth silicate microsphere in air, showing the electric field profile in (a) the r - θ plane (cross-section view) and (b) the r - ϕ plane (equatorial-section view) at the equator where r , ϕ and θ are the radial, azimuthal, and polar spherical axes. Parameters: mode order numbers are $l=m=673$ and $n=5$, TE mode, the operating wavelength is 1550 nm and the microsphere diameter $D = 179 \mu\text{m}$.

To date, thermal effects in highly integrated photonic circuits are one of the major issues contributing to their high energy consumption and introducing unwanted thermal nonlinearities. Also, such temperature fluctuations are transformed into wideband noise in output channels because of the temperature dependence of device parameters, especially for a photonic device with a small volume such as microresonator. Therefore, it is necessary to investigate such thermal effects induced by absorption for future research in the area. Figure 3 shows the temperature dependence of the resonance wavelengths λ_R for a $179 \mu\text{m}$ diameter microsphere. The red shifting of λ_R with higher T is mediated by an increase in both the microsphere size and refractive index - the two contributions being additive - and since the thermal expansion coefficient ($\epsilon \sim 1 \times 10^{-5} / ^\circ\text{C}$) and the thermo-optic coefficient ($dn_s/dt = 2.2 \times 10^{-5} / ^\circ\text{C}$) [16] of bismuth silicate are similar in magnitude, it is necessary to incorporate both effects when solving the WGM eigenvalue equation. Despite the difference between the modes' field distributions, their resonance shift gradients are almost the same at $d\lambda_R/dT = 32 \text{ pm}/^\circ\text{C}$ and close to the linearised approximation

$$\Delta\lambda_R/\Delta T \approx \varepsilon + (dn_s/dt)/n_s [17].$$

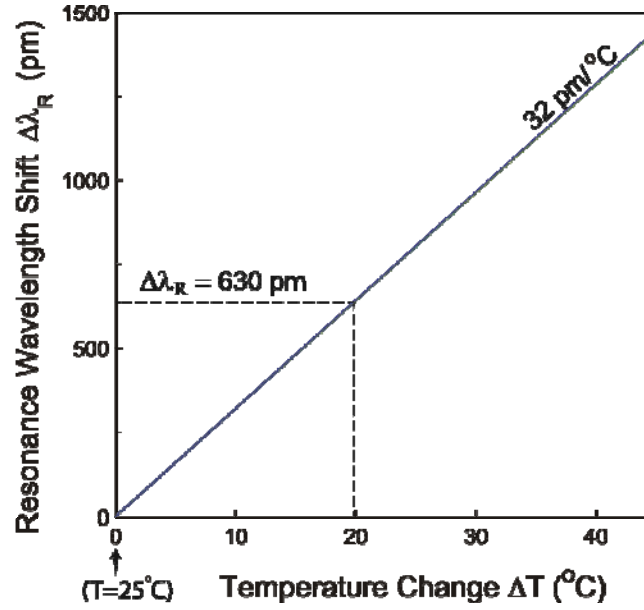


Figure 3. Theoretical thermally-induced resonance wavelength shift of 6 WGMs, with radial orders $n=1\sim6$ and $l = m$ chosen such that the resonance wavelengths are near 1550 nm. Sphere diameter is 179 μm .

3. Fabrication of bismuth silicate microsphere

The microsphere was fabricated from a highly nonlinear fiber manufactured by Asahi Glass Ltd (Japan), which had core and cladding diameters of 6.9 μm and 125.6 μm , and core and cladding refractive indices (at $\lambda\sim1550$ nm) of 2.02 and 2.01, respectively. The fiber had a nonlinear refractive index of $n_2=3.2\times10^{-19}$ m^2/W [11], which is ~17 times larger than that of silica.

To fabricate small bismuth-silicate microspheres, the bismuth-silicate fiber was first tapered using the modified “flame brushing technique” [18]. This technique involves scanning a microheater over a fiber being stretched. As shown in Fig. 4b, a small region of the fiber is heated by the resistive microheater with a “ Ω ” shape at a temperature of ~500 °C. The resulting tapers had a uniform waist diameter of $d<5$ μm . After tapering, the uniform waist region (~5 mm long) was then cut in the center (Fig.

4c). The tip of the taper was then heated to about 900 °C, which is significantly higher than the softening point (510 °C) of the bismuth silicate glass, and the surface tension of the softened bismuth-silicate glass molded the tip into a spherical shape.

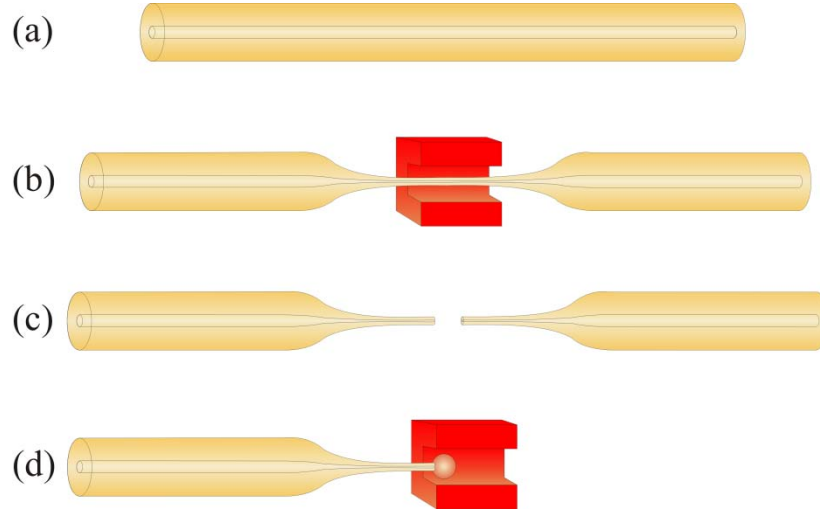


Figure 4. Schematic diagram illustrating the fabrication of microspheres from bismuth-silicate fibers: (a) a bismuth-silicate glass fiber (NA~0.2, V~2.81) (b) the bismuth-silicate fiber is tapered to a waist diameter $d < 5 \mu\text{m}$ over a length of ~5 mm by using a resistive microheater at a temperature of ~500 °C; (c) the taper is cut in the middle; (d) a microsphere is formed at the taper tip when the tip approaches the microheater maintained at about 900 °C, which is significantly higher than the softening point of bismuth-silicate glass (~510 °C).

4. Measurement of the bismuth silicate glass microsphere

The experimental apparatus used for optical characterization of the bismuth silicate microsphere is shown in Fig. 5. Light from a narrow-line tunable laser source (Agilent 81600B, Wavelength resolution: 0.1 pm, Relative wavelength accuracy: typ. ± 2 pm, Agilent, Santa Clara, CA, USA) emitting a power range from 0.1 mW (-10 dBm) to 6.31 mW (8 dBm) over the wavelength range 1540 nm to 1560 nm was launched into a tapered silica fiber and coupled to the bismuth silicate microsphere. The throughput signal was collected using an InGaAs photodetector. The separation between the microsphere and the tapered fiber was controlled with a precision

nanotranslation stage equipped with piezoelectric actuators and stepper motors and monitored using a microscope equipped with a CCD camera. The tapered fiber stem supporting the microsphere ensured that the microsphere orientation remained fixed with respect to the tapered silica coupling fiber as it was translated across and away from it. In the experiments, we set the separation to zero between the microsphere and taper so they touched to maximize the resonance intensity over the entire wavelength range and, above all to ensure mechanical stability over the whole measurement duration.

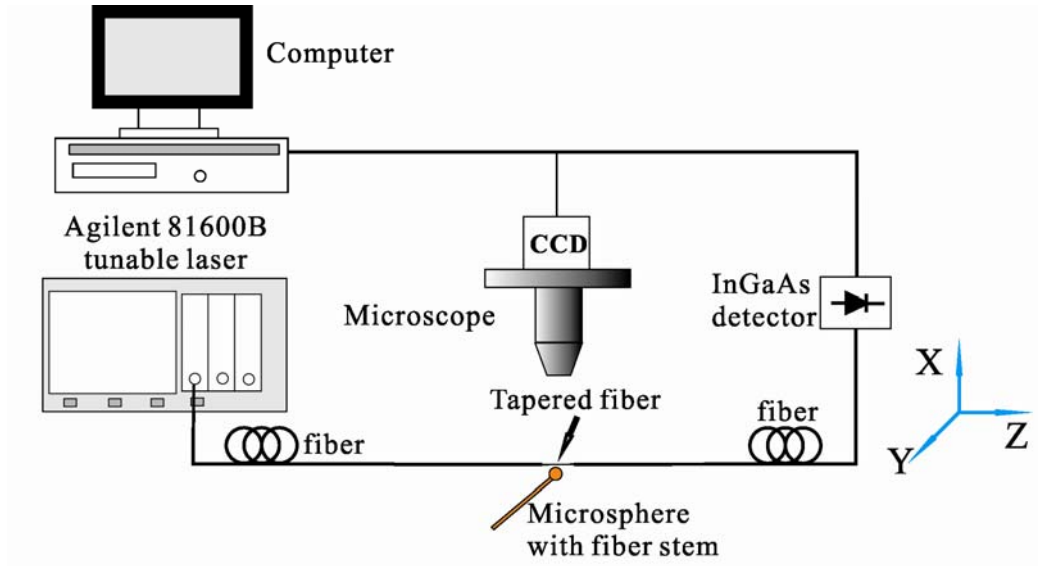


Figure 5. Experimental apparatus used for microsphere resonance characterization.

Fig. 6(a) shows the top view of the bismuth-silicate glass microsphere resonator with a diameter of $179\ \mu\text{m}$, in close proximity to a tapered silica fiber with a waist diameter $d \sim 2\ \mu\text{m}$. Fig. 6(b) and (c) show CCD images when the input light is off and on, respectively. The CCD camera is sensitive to the $1550\ \text{nm}$ radiation and Fig 6(c) clearly shows scattered light from a WGM. There is also some evidence of leakage into the stem, possibly due to the wide-spread higher-order angular modes associated with the ellipticity in the microsphere. At resonant wavelengths up to about 94% of the light in the fiber taper was coupled into the microsphere. The power transmitted through the excitation fiber taper was recorded as a function of wavelength at input

powers ranging from 0.1 mW to 6.3 mW.

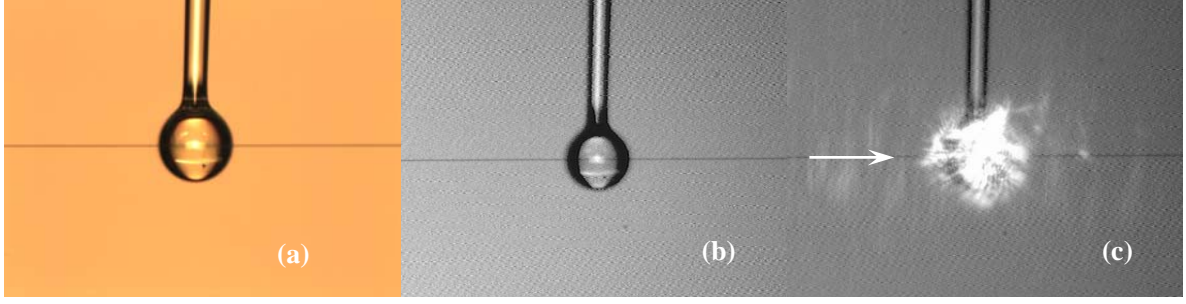


Figure 6. Microscope images of bismuth-silicate microspheres with a diameter (a) $179\text{ }\mu\text{m}$ showing its fiber stem and the tapered coupling fiber. (b) and (c) show the infrared CCD images of the microsphere when the input laser light is turned off and on, respectively.

5. Experimental results and discussion

Dips in power transmission through the tapered coupling fiber are observed by the InGaAs detector as a function of wavelength when good coupling to the microsphere is achieved. Figure 7 shows resonance spectra of the microsphere with a diameter of $179\text{ }\mu\text{m}$, over wavelength ranges of (a) 20 nm and (b) 3 pm , with an input power of -10 dBm (0.1 mW). It is evident from the figure that the tapered fiber excitation produces dense spectral features as experienced in other high index glass microspheres [3,5]. This is due to the excitation of many higher-order radial modes by the low effective index fiber taper and many non-degenerate higher-order angular modes associated with microsphere ellipticity [19]. As shown in Fig. 1, the first 6 radial modes ($n=1\sim6$) for a bismuth-silicate microsphere of about $180\text{ }\mu\text{m}$ diameter at a wavelength of 1550 nm have effective indices varying from 1.97 to 1.84, while the effective index of the fundamental mode in a $2\text{ }\mu\text{m}$ tapered fiber at the same wavelength is approximately 1.35. For this reason, the taper will not excite prevalently a single mode in the microsphere, but will excite a wealth of modes, as shown in Fig. 7(a). In this study, a tapered silica fiber (instead of a phase-matched tapered high index fiber) was used to excite WGMs, mainly to minimize any nonlinear effects from the delivery fiber.

The Q of a microsphere resonator can be easily estimated from its WGM spectrum through the relation, $Q=\lambda/\Delta\lambda$, where $\Delta\lambda$ is the full width at half maximum (FWHM) and λ is the central wavelength of the resonance. Fig. 7(b) presents the spectrum over a short wavelength range, showing the high Q nature of the observed resonance dips. Resonances with FWHM in the region of 0.26 pm (50 MHz) have been observed, resulting in a Q factor of 0.6×10^7 . This measured Q factor is close to the theoretical limit (1.77×10^7 at $\lambda\sim 1550$ nm) predicted using the equations reported in Ref. [2] for a pure bismuth silicate glass using an optical attenuation of 4.6×10^{-3} cm⁻¹ (~ 2 dB/m) and a refractive index of $n_{1550}=2.01$. The difference is mainly due to the scattering loss from surface roughness. Both the absorption and scattering loss of bismuth silicate microsphere are much higher than those for pure silica [2].

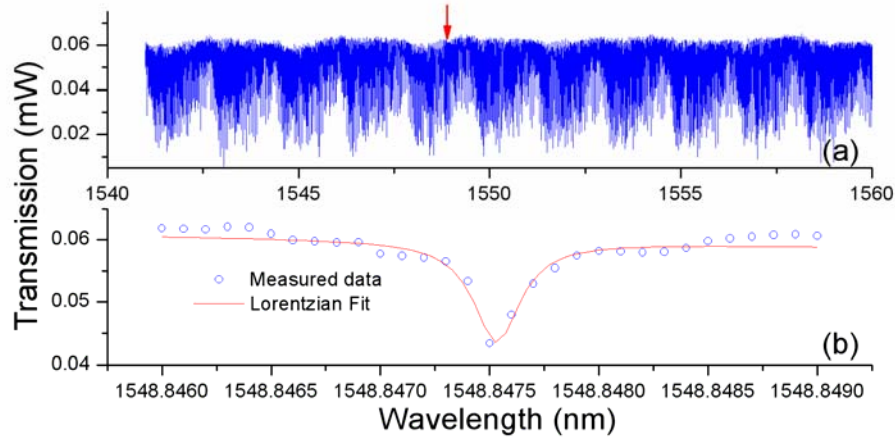


Figure 7. (a) Experimental resonance spectra for wavelengths between 1540 nm and 1560 nm for the microsphere with diameter 179 μ m; (b) Close-up spectrum in the region 1548.846 - 1548.849 nm: the high- Q resonance (circles) is approximated by a Lorentzian fit to accurately determine the bandwidth.

Here, the dependence of the microsphere WGMs spectrum on the input power was investigated. Fig. 8 shows the transmission spectra obtained between 1547.1 nm and

1548.3 nm for input power levels between 0.1 mW and 6.3 mW. In experiments, increasing the input CW power from 0.1 mW (-10 dBm) to 6.31 mW (8 dBm) shifted the resonance wavelength by 627 pm and 633 pm respectively for peaks 1 and 2 (identified in Fig. 8). In Fig. 9, these resonance wavelengths are also plotted as a function of the input power. The tunable laser used in the tests had a wavelength positioning accuracy of about ± 1 pm, which is indicated as error bars in Fig. 9; each experimental point has been measured with the same accuracy.

While at lower powers WGM peaks are easily resolved in Fig. 8, at higher powers strong attenuation over broad wavelength regions is observed. It is reasonable to assume that the temperature increases with circulating power due to residual absorption, while the circulating power increases with increasing input power when the wavelength is close to a resonance. The coefficient of thermal expansion and the thermal coefficient of refractive index are both positive in bismuthate glasses [15] so a temperature increase should cause a red-shift in WGM resonance wavelengths. Indeed, shifts in the resonant wavelengths with increasing circulating power due to thermal effects have been investigated previously [17, 20, 21]. The broad attenuation is probably due to the contribution of several effects, which might include optical nonlinearities (Kerr effect), thermal shift and temperature oscillations during the measurement. Multiple scanning through all the resonances which are situated within the whole scanned wavelength region, increase the microsphere temperature because of absorption which changes both the microsphere refractive index and geometry. As shown in the Fig. 8, small oscillations attributed to the Andronov-Hopf bifurcation can be clearly seen on the spectral responses when the input power is 6.3 mW and 3.16 mW. The experimentally observed resonance shift of ~ 630 pm at 6.3 mW input power implies that the microsphere temperature increases by approximately $\Delta T \sim 20^\circ\text{C}$ near resonance. This value is considered as an upper limit since the Kerr nonlinearity may also red shift the resonance, especially given the high Q factor. It is also interesting to note experimentally, as shown in Fig. 8, the difference between $\Delta\lambda_R$ for peaks 1 and 2 varies up to 7 pm. This may be due to different circulating cavity power and hence temperature between the two peaks resonances, owing, for example, to surface

scattering or external coupling effects which would affect higher order modes more noticeably.

However, Fig. 9 also shows the resonance wavelength shift is only significant for powers exceeding 0.8 mW; below this value the thermally induced redshift due to absorption is negligible which makes it possible to apply fairly high powers without adverse thermally-induced refractive index changes in the bismuth silicate microsphere. This is particularly beneficial for nonlinear optical applications in which performance is often subject to thermal limitations, with the potential to implement robustly assembled fully integrated all-optical switching devices [22].

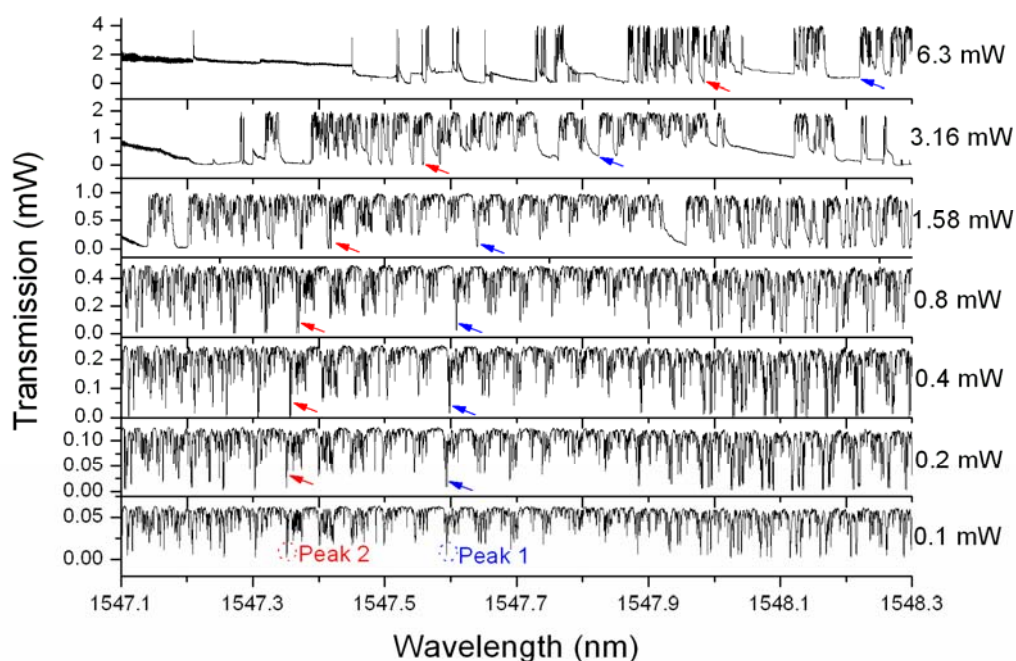


Figure 8. Experimental transmission spectra obtained with the input power varying from 8 dBm to -10 dBm: Peak 1@ 1547.5937 nm and Peak 2@1547.3514 nm are marked by blue and red arrow, respectively.

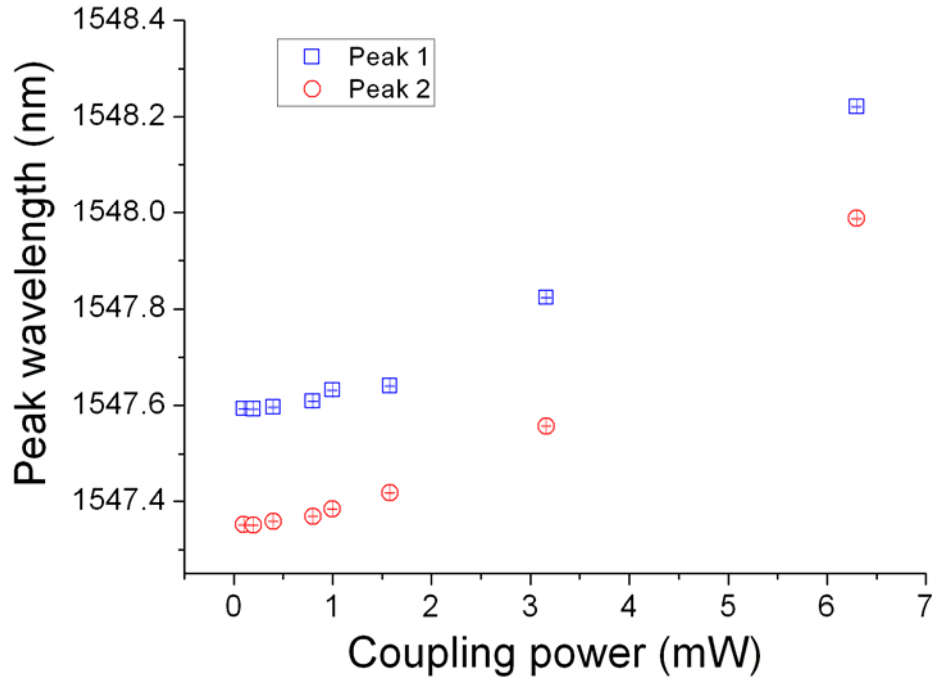


Figure 9. Thermal shift of the high-Q resonances ($\lambda_{\text{resonance}} = 1547.5937$ nm and 1547.3513 nm for peak 1 and peak 2 at 0.1mW, respectively) depending on coupling power.

6. Conclusion

In conclusion, the fabrication of bismuth-silicate glass microspheres has been demonstrated. Whispering gallery mode resonances excited by evanescent coupling from a silica fiber taper with a diameter $d \sim 2 \mu\text{m}$ have been observed and a high Q factor up to 0.6×10^7 was recorded at $\lambda \sim 1550$ nm. Thermal effects have been investigated both theoretically and experimentally. It is anticipated that such a bismuth silicate microsphere can provide an ideal building-block for several applications including highly integrated optical switches, modulators, ultrasmall optical filters, microlasers, and optical biosensors. Work is underway to realize nonlinear optical performances involving this nonlinear microsphere with a low-threshold, such as Raman scattering and four-wave mixing.

P. Wang is funded by the Irish Research Council for Science, Engineering and

Technology, co-funded by the Marie-Curie Actions under FP7. G. Brambilla gratefully acknowledges the Royal Society (London) for his research fellowship. Q. Wu gratefully acknowledges the support of Science Foundation Ireland under grant no. 07/SK/I1200.

References:

- [1]. J. S. Wilkinson, G. S. Murugan, D. W. Hewak, M. N. Zervas, Y. Panitchob, G. R. Elliott, P. N. Bartlett, E. J. Tull, K. R. Ryan, "Integrated microsphere planar lightwave circuits", European Conference on Integrated Optics 2010 Cambridge 7-9 Apr 2010 ThB3.
- [2]. M. L. Gorodetsky, A. A. Savchenkov, and V. S. Ilchenko, "Ultimate Q of optical microsphere resonators," *Opt. Lett.*, Vol. 21, No. 7, pp. 453-455, (1996).
- [3]. G. R. Elliott, D.W. Hewak, G. Senthil Murugan and J.S. Wilkinson, "Chalcogenide glass microspheres; their production characterization and potential," *Optics Express*, 15, 17542, (2007).
- [4]. C. Grillet, S. N. Bian, E. C. Magi, and B. J. Eggleton, "Fiber taper coupling to chalcogenide microsphere modes," *Appl. Phys. Lett.*, Vol, 92, 171109, 2008.
- [5]. P. Wang, G. S. Murugan, T. Lee, X. Feng, Y. Semenova, Q. Wu, W. Loh, G. Brambilla, J. S. Wilkinson and G. Farrell, "Lead silicate glass microsphere resonators with absorption-limited Q," *Appl. Phys. Lett.*, 98, 181105, 2011.
- [6]. M. J. Weber, *Handbook of Optical Materials*, CRC Press, (2003).
- [7]. N. Sugimoto, H. Kanbara, S. Fujiwara, K. Tanaka, Y. Shimizugawa, and K. Hirao, "Third-order optical nonlinearities and their ultrafast response in Bi_2O_3 - B_2O_3 - SiO_2 glasses," *J. Opt. Soc. Am. B*, 16, 1904-1908 (1999).
- [8]. Y. Kuroiwa, N. Sugimoto, K. Ochiai, S. Ohara, Y. Furusawa, S. Ito, S. Tanabe, and T. Hanada, "Fusion spliceable and high efficient Bi_2O_3 -based EDF for short length and broadband application pumped at 1480 nm," presented at OFC 2001, Anaheim, California, USA, 2001, paper TuI5.
- [9]. G. Brambilla, F. Koizumi, V. Finazzi, and D. J. Richardson, "Supercontinuum generation in tapered bismuth silicate fibres," *Electron. Lett.*, vol. 41, pp. 795-797, 2005.
- [10]. G. Brambilla, J. Mills, V. Finazzi, and F. Koizumi, "Long-wavelength supercontinuum generation in bismuth-silicate fibres," *Electron. Lett.* 42, 574-575 (2006).
- [11]. J. H. Lee, T. Nagashima, T. Hasegawa, S. Ohara, N. Sugimoto, and K. Kikuchi, "Bismuth-Oxide-Based Nonlinear Fiber With a High SBS Threshold and Its Application to Four-Wave-Mixing Wavelength Conversion Using a Pure Continuous-Wave Pump," *J. Lightwave Technol.* 24, 22-28 (2006).
- [12]. K. K. Qureshi, H. Y. Tam, W. H. Chung, P. K. A. Wai, N. Sugimoto, "All optical on-off switching using bismuth-based highly nonlinear fiber," in *Proc. Conf. Lasers and Electro-Optics (CLEO)*, Long Beach, USA, May 21-26, 2006, paper CMAA2.
- [13]. I. V. Kabakova, Dan Grobnc, Stephen Mihailov, Eric C. Mägi, C. Martijn de Sterke, and Benjamin J. Eggleton, "Bragg grating-based optical switching in a bismuth-oxide fiber with strong $\chi(3)$ -nonlinearity," *Opt. Express*, 19, 5868-5873 (2011).
- [14]. M. Jamshidifar, A. Vedadi, D. S. Govan, M.E. Marhic, Continuous-wave parametric amplification in bismuth-oxide fibers, *Optical Fiber Technology*, 16, 6,

- p. 458-466 (2010).
- [15]. B. E. Little, J. P. Laine and H. A. Haus, "Analytic Theory of Coupling from Tapered Fibers and Half-Blocks into Microsphere Resonators," *J. Lightwave Technol.*, 17, 704 (1999).
 - [16]. A. Koike and N. Sugimoto, "Temperature Dependences of Optical Path Length in Inorganic Glasses," *Reports Res. Lab. Asahi Glass Co., Ltd.*, 56, 1-6 (2006).
 - [17]. T. Carmon, L. Yang, and K. J. Vahala, "Dynamical thermal behavior and thermal self-stability of microcavities," *Opt. Express* 12, 4742-4750 (2004).
 - [18]. G. Brambilla, F. Koizumi, X. Feng, and D. J. Richardson, "Compound-glass optical nanowires," *Electron. Lett.* 41, 400-402 (2005).
 - [19]. G. S. Murugan, Y. Panitchob, E. J. Tull, P. N. Bartlett, D. W. Hewak, M. N. Zervas, and J. S. Wilkinson, "Position-dependent coupling between a channel waveguide and a distorted microsphere resonator," *J. Appl. Phys.*, 107, 053105 (2010).
 - [20]. M. Soltani, Q. Li, S. Yegnanarayanan, and A. Adibi, "Improvement of thermal properties of ultra-high Q silicon microdisk resonators," *Opt. Express* 15(25), 17305–17312 (2007).
 - [21]. K. Ikeda, R. E. Saperstein, N. Alic, and Y. Fainman, "Thermal and Kerr nonlinear properties of plasma-deposited silicon nitride/ silicon dioxide waveguides," *Opt. Express* 16(17), 12987–12994 (2008).
 - [22]. V. R. Almeida, C. A. Barrios, R. R. Panepucci, & M. Lipson, "All-optical control of light on a silicon chip," *Nature* 431, 1081–1084 (2004).